SEGMENTATION OF MR IMAGE BASED ON MAXIMUM *A POSTERIOR*

F. Liu, S. Gao, X. Gao
Institute of Biomedical Engineering, Dept. of Electrical Engineering,
Tsinghua University, Beijing 100084, P. R. China

Abstract- **Brain MR image segmentation takes an important role in research and clinical application. Statistical method is effective in the segmentation, which is usually based on maximum *a posteriori* (MAP). The key of MAP method is to estimate *a prior* probability of the segmentation. Multilevel logistic (MLL) model has been used in practice for the estimation. To farther improve the performance of the segmentation, a weighted MLL (WMLL) model is proposed in this paper. The simulated results show that the WMLL model is effective.**

***Keywords* - MR image, image segmentation, MLL model.**

I. INTRODUCTION

Brain MR image segmentation takes an important role in clinical applications. It is well known that manual segmentation of such images is not only tedious but also inconsistent. So automatic or semi-automatic methods are desirable. Hitherto many methods have been developed, which can be categorized into three classes [1], which are based on region [2]-[5], boundary[6]-[8], and point[9]-[17] respectively. The method based on region is computationally effective due to the split and merge algorithm provided by Horowitz and Pavlidis [2], but it has difficulty in getting a unique result [3]. Sonka [4] segments images into small pieces and then applied genetic algorithm to rearrange them, so that they form large regions consisting with prior knowledge, which is obtained from manually segmented images. However, it seems not easy to generalize such method to other cases. Those methods based on boundary fail to sufficiently utilize all messages in images. The segmentation method based on point can be found in many literatures recently. Various techniques have been adopted, including fuzzy [9], neural networks, genetic methods [10][11], statistical [12]-[17] and so on.

The statistical approach is paid much more attentions in present study, particularly those based on maximum *a posteriori* (MAP) methods. In statistical methods, the prior probability of the segmentation is not easy to estimate. So maximum likelihood (ML) method is applied in some literature [17], which only considered $p\{y|x\}$, where y represents intensities of an image and x the segmentation. But ML method is liable to violate the piecewise congruous of tissues [17]. As Markov random field (MRF) and Gibbs distribution (GD) equivalence [12] was introduced, prior distribution of the segmentation can be calculated. Multilevel logistic (MLL) model is a typical way to do so. To further improve the performance of the segmentation, a weighted MLL (WMLL) model is proposed in this paper.

II. WEIGHTED MULTILEVEL LOGISTICS MODEL

There exist three main obstacles in segmentation of brain MR images [17]: the thermal or electronic noise, the intensity non-uniformity of same tissue classes, and the partial volume effects. Thermal noise is often assumed Gaussian, white, additive, and tissue dependent. Intensity non-uniformity of same tissues is due to biological variance in different structures of the same tissue and irregularities in imaging equipment. It is assumed slowly varied spatially. Partial volume effects are due to the limited resolution of MR images. Thermal noise and identity non-uniformity are studied in present research, but the partial volume effects are left unconsidered.

Let $y=\{y_i \ ; \ i \in I\}$ be an image in Cartesian space N^2, where $I \in N^2$ is the region that y occurs. y_i is the intensity of the image at site i. y can be regard as a realization of analog random variables at I. Suppose there are K different tissues (classes) in the image, and each of them is labeled by a number in $\Lambda=\{1,2,...K\}$. Let $x_i=k$，$k \in \Lambda$ indicates that site i belongs to class k, then $x=\{x_i \ ; \ i \in I\}$ denotes a segmentation of y. x can also be regarded as a realization of discrete random variables at I. The goal of image segmentation is to find an optimal or sub-optimal x under some principle.

In MAP method, $P\{x|y\}$ is considered and the optimal $x=x^*$ that makes it largest is regarded as the segmentation result. Usually by Bayes' theorem it can be written in the following form

$$P\{x \mid y\} = \frac{p\{y \mid x\}P\{x\}}{p\{y\}} \propto p\{y \mid x\}P\{x\} \tag{1}$$

So the problem is transferred to finding maximum product of $p\{y|x\}$ and $P\{x\}$.

$p\{y|x\}$ is the joint density function of $y=\{y_1, y_2, ..., y_{|I|}\}$ under segmentation x, where $|I|$ is the total number of sites in image y. y_i is assumed disturbed by additive, white, Gaussian, tissue dependent, and space variant noise, so if $x_i=k$, then

$$y_i = \mu_{i,k} + n_{i,k} \tag{2}$$

where μ_{ik} is the mean intensity of tissue k at site i, and n_{ik} is Gaussian noise at i corresponding to tissue k, whose density function obeys $N(0, \sigma_{ik}^2)$. Since the noise in the image is a space-variant white Gaussian process and tissue dependent, they are conditionally independent [17]. Let R_k be the set of sites that belong to class k, then $p\{y|x\}$ can be expressed as

$$\begin{aligned} P\{y \mid x\} &= \prod_{k=1}^{K}\prod_{i \in R_k} \frac{1}{\sqrt{2\pi}\sigma_{k,i}} \exp\left\{-\frac{1}{2}\left(\frac{y_i-\mu_{k,i}}{\sigma_{k,i}}\right)^2\right\} \\ &= \frac{1}{(2\pi)^{|I|/2}} \exp\left\{-\sum_{k=1}^{K}\sum_{i \in R_k}\left(\ln(\sigma_{k,i}) + \frac{1}{2}\left(\frac{y_i-\mu_{k,i}}{\sigma_{k,i}}\right)^2\right)\right\} \end{aligned} \tag{3}$$

where all of parameter pairs $\theta_i = \{(\mu_{ik}, \sigma_{ik}); k \in \Lambda\}$ form a parameter set $\theta = \{\theta_i; i \in I\}$.

MLL model is an effective way to estimate $P\{x\}$ by using information of the segmentation x itself. However, it still has some disadvantages due to its assumption of homogeneity of

Report Documentation Page

Report Date	Report Type	Dates Covered (from... to)
25 Oct 2001	N/A	-

Title and Subtitle Segmentation of MR Image Based on Maximum A Posterior	**Contract Number**
	Grant Number
	Program Element Number
Author(s)	**Project Number**
	Task Number
	Work Unit Number
Performing Organization Name(s) and Address(es) Institute of Biomedical Engineering Dept of Electrical Engineering Tsinghua University Beijing 100084, P.R. China	**Performing Organization Report Number**
Sponsoring/Monitoring Agency Name(s) and Address(es) US Army Research, Development & Standardization Group (UK) PSC 803 Box 15 FPO AE 09499-1500	**Sponsor/Monitor's Acronym(s)**
	Sponsor/Monitor's Report Number(s)

Distribution/Availability Statement
Approved for public release, distribution unlimited

Supplementary Notes
Papers from 23rd Annual International Conference of the IEEE Engineering in Medicine and Biology Society, October 25-28, 2001, held in Istanbul, Turkey. See also ADM001351 for entire conference on cd-rom., The original document contains color images.

Abstract

Subject Terms

Report Classification unclassified	**Classification of this page** unclassified
Classification of Abstract unclassified	**Limitation of Abstract** UU

Number of Pages
4

the images. For example, different segmentations may have the same prior probability according to the model. In fact, since white matter (WM) is always surrounded by gray matter (GM) in brain MR images, any estimation of the prior probability of segmentations that WM is outside of GM should be zero, or at least very small, which is not the case in MLL model. This implies that the assumption of homogeneous is not acceptable in brain MR image segmentations.

In practice, computation burden is so large that images are segmented site by site [17]. So for site *i*, the probability of $x_i=k$ is

$$\begin{aligned} P\{x_i = k \mid y_i, x_j, j \neq i\} &= P\{x_i = k \mid y_i, x_j, j \in \eta_i\} \\ &\propto p\{y_i, x_j, j \in \eta_i \mid x_i = k\} P\{x_i = k\} \\ &= p\{y_i \mid x_i = k\} P\{x_j, j \in \eta_i \mid x_i = k\} P\{x_i = k\} \\ &= p\{y_i \mid x_i = k\} P\{x_i = k, x_j, j \in \eta_i\} \\ &= p\{y_i \mid x_i = k\} P_k\{x_i\} \end{aligned} \tag{4}$$

provided that yi and xj's are conditionally independent, where η_i is the neighborhood of *i*, which does not contain *i* itself, and $P_k\{x_i\}$ denotes $P\{x_i=k, x_j, j \in \eta_j\}$.

In MLL model, $P_k\{x_i\}$ is calculated as

$$P_k\{x_i\} = \frac{1}{Z}\exp\left\{-\sum_{i\in c} V_c(x)\right\} \tag{5}$$

where *c* is a clique, $V_c(x)$ is the potential of clique *c*, and *Z* is the normalization constant. But real images may not be MRF, so estimating $P_k\{x_i\}$ using (5) may produce errors.

In our study, $P_k\{x_i\}$ is weighted by the probability of class *k* at site *i* in order to get better estimation. Suppose that $\pi_k\{x_i\}$ be the probability of class *k* at site *i*, then $P_k\{x_i\}$ can be written as

$$P_k'\{x_i\} = \frac{1}{Z'}\exp\left\{-\sum_{i\in c} V_c(x)\right\}\pi_k\{x_i\} \tag{6}$$

where Z' is the normalization constant.

Let t' be classifications of sites in η_i, then $V_c(x)$ is exactly determined by x_i and t', since in (5) or (6), $i \in c$. So $V_c(x)$ is just $V_c(x_i, t')$. Thus the normalization constant can be expressed as

$$Z' = \sum_{x_i=1}^{K}\sum_{t'\in\Omega'}\exp\left\{-\sum_{i\in c} V_c(x_i, t')\right\}\pi_k\{x_i\} \tag{7}$$

where Ω' is the space of t'. Since normalization constant does not affect classification, it is denoted by *Z* for simplicity in the context, despite that it may have different expressions. So $P\{x_i=k \mid y_i, x_j, j\neq i\}$ can be written as

$$\begin{aligned} P\{x_i = k \mid y_i, x_j, j \neq i\} &\propto p\{y_i \mid x_i = k\} P_k\{x_i\} \\ &= \frac{1}{\sqrt{2\pi}\sigma_{k,i}}\exp\left(-\frac{1}{2}\left(\frac{y_i-\mu_{k,i}}{\sigma_{k,i}}\right)^2\right)\frac{1}{Z}\exp\left(-\sum_{i\in c} V_c(x)\right)\pi_k(x_i) \\ &= \frac{1}{\sqrt{2\pi}Z}\exp\left(-\left(\log(\sigma_{k,i}) + \frac{1}{2}\left(\frac{y_i-\mu_{k,i}}{\sigma_{k,i}}\right)^2 + \sum_{i\in c} V_c(x) - \log(\pi_k(x_i))\right)\right) \\ &= \frac{1}{\sqrt{2\pi}Z}\exp(-U_k(x_i)) \end{aligned} \tag{8}$$

where

$$U_k(x_i) = \left(\log(\sigma_{k,i}) + \frac{1}{2}\left(\frac{y_i-\mu_{k,i}}{\sigma_{k,i}}\right)^2 + \sum_{i\in c} V_c(x) - \log(\pi_k(x_i))\right) \tag{9}$$

Usually $\pi_k\{x_i\}$ is not known except that many accurately segmented images are statistically analyzed. To overcome this obstacle, intensities of the image are involved in estimating $\pi_k\{x_i\}$. Since class *k* has a mean intensity $\mu_{k,i}$ at site *i*, *k=1,2,...K*, it is natural to assume that the closer y_i is to $\mu_{k,i}$, the more possible that it belongs to class *k*, and the larger probability of class *k* at site *i*. An instinct way of describing "closeness" is to adopt intensity Euclidean distance measure, which is the absolute value of difference between two intensities. Thus, the larger the intensity Euclidean distance between y_i and $\mu_{k,i}$, the smaller probability of $\pi_k\{x_i\}$. So

$$\pi_k\{x_i\} = \frac{1}{Z}\frac{1}{|y_i-\mu_{k,i}|} \tag{10}$$

Images are usually corrupted by thermal noise, as described before, intensity of a single site may be distorted too much that it cannot correctly reflect intensity Euclidean distance. So a misclassification may occur. To solve this problem, two methods can be applied. The first one is to decrease effect of noise in calculating $\pi_k\{x_i\}$; the second one is to add threshold in the judgment step of the algorithm.

To decrease effect of noise in calculating $\pi_k\{x_i\}$, $|y_i-\mu_{k,i}|$ in (8) is replaced by $\overline{|y_i-\mu_{k,i}|}$, which is the mean value of $|y_j-\mu_{k,i}|, j\in Q_i'$, where Q_i' is a neighbor region of site *i*. So

$$\pi_k\{x_i\} = \frac{1}{Z}\frac{1}{\overline{|y_i-\mu_{k,i}|}} \tag{11}$$

This method holds provided that the spatial probability distribution of each class is a smooth surface.

A threshold q_i' can be applied to decrease occurrence of the misclassification either. Since classes are piecewise contiguous, if site *i* belongs to some class *k*, there should be some sites in its neighborhood η_i that also belongs to class *k*. if not, site *i* should not be classified as class *k*. q_i' takes the role of checking whether there is enough sites that belong to class *k*.

The above estimation does not include noise model in images, at least it does not care standard variance. In fact, since noise is assumed to be white and Gaussian, this model can be applied in estimating probability of class *k* at site *i*. In this case, the probability of class *k* at site *i* has the following form:

$$\pi_k\{x_i\} = \frac{1}{Z}\frac{1}{\sqrt{2\pi}\sigma_{k,i}}\exp\left(-\frac{1}{2}\left(\frac{|y_i-\mu_{k,i}|}{\sigma_{k,i}}\right)^2\right) \tag{12}$$

For the same reason shown above, to prevent effect of large noise at some sites, $|y_i-\mu_{k,i}|$ in (12) can be replaced by

$\overline{|y_i - \mu_{k,i}|}$, or threshold can be introduced, as is done when only intensity Euclidean distance is applied.

$$\pi_k\{x_i\} = \frac{1}{Z}\frac{1}{\sqrt{2\pi}\sigma_{k,i}}\exp\left(-\frac{1}{2}\left(\frac{\overline{|y_i - \mu_{k,i}|}}{\sigma_{k,i}}\right)^2\right) \quad (13)$$

Also (13) holds provided that the spatial probability distribution of each class is a smooth surface

III. Segmentation Algorithm

Iterated conditional modes (ICM) proposed by Beseg [13] is applied to segment images [17]. This procedure is also applied in our study. The key point of ICM in the study is to estimate parameters in MLL model from current segmentation result [14], then classifying the image site by site, then use the new segmentation result to estimate MLL model parameters, and so on. This procedure continues until some criterion is satisfied, say, maximum loop time is reached or the change between two recent segmentations is ignorable.

Before $U_k(xi)$ is calculated, parameter set θ should be known. It can be obtained by taking sample means and deviations of intensities of those sites belonging to class k in neighbor region Q_i of site i. In case that there are not enough sites belonging to some class k in Q_i, class k is regarded as not existed at site i. So a threshold q_i is set so that any class with less than q_i sites belonging to it in Q_i cannot be assigned to x_i.

IV. Results

Brain MR images are downloaded from brainweb [18]. The size of McGill data is 181*217*181 with voxel size of 1*1*1 mm^3, from which the 94th slice is randomly selected for segmentation. McGill provides two sets of images with different noise disturbance and intensity non-uniformity. One is corrupted by 3% noise with 20% intensity non-uniformity, and the other is corrupted by 9% noise with 40% intensity non-uniformity. The later is adopted to check the WMLL model.

Since the destination of segmentation in this study is to separate GM and WM, tissues like skin, skull and others are roughly pre-eliminated by a template before segmentation. According to intensity histogram, four kinds of tissues exist in the remaining image. To speed up the segmentation process and avoid background interference in the process, sites outside of the template are kept from the process. Neighbor region Q_i of site i is 41*41, and Q_i' is also 41*41 although they are not necessarily be the same. q_i = 8 and q_i' = 0,1,2 respectively.

Fig.1. shows the results of the segmentation using different $\pi_k(x_i)$s described in section II. (a) is the original corrupted image and (b) is the intensity histogram of (a). (c)-(e) show the results when (10) is adopted with q_i' = 0,1,2 respectively; (f) shows result when (11) is adopted; (g)-(i) show results when (12) is adopted with q_i' = 0,1,2 respectively; and (j) shows result when (13) is adopted. The corresponding covariance coefficients of WM and GM are given in Table 1.

IV. Discussion and Conclusion

In statistical segmentation methods, MLL model is not fully acceptable in brain MR image segmentation. In this

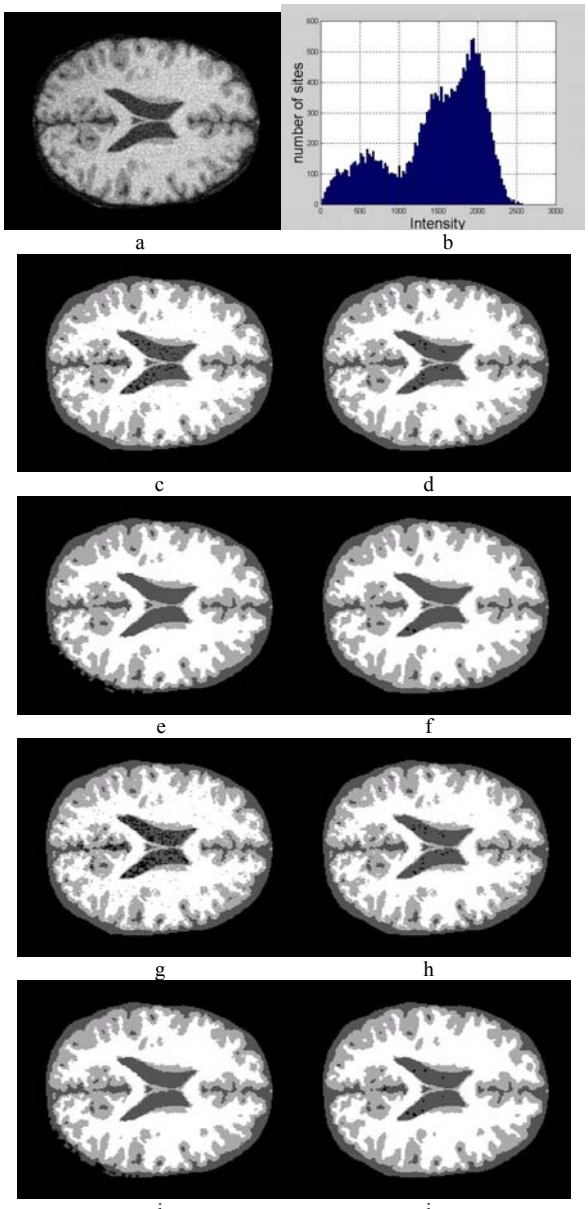

Fig.1. Results when different expression of $\pi_k(x_i)$ is adopted. (a) Original corrupted image. (b) Intensity histogram of (a). (c)-(e) (11) is adopted with q_i' being 0,1,2 respectively. (f) (12) is adopted. (g)-(i) (13) is adopted with q_i' being 0,1,2 respectively. (j) (14) is adopted.

TABLE I
COVARIANCE COEFFICIENTS OF GM AND WM

$\pi_k(x_i)$	(10)			(11)	(12)			(13)
q_i'	0	1	2	0	0	1	2	0
GM	0.9037	0.9057	0.9133	0.9186	0.8805	0.8920	0.9111	0.9198
WM	0.9289	0.9287	0.9312	0.9395	0.9189	0.9223	0.9269	0.9390

paper, WMLL is used to further improve the performance of the segmentation. Two methods of weight estimation are provided. (11) and (13) hold provided that the spatial probability distribution of each tissue is smooth. Since the segmentation results are better than others when (11) and (13) are adopted, it seems that the assumption is correct according to our limited experiments. If only $|y_i - \mu_{k,i}|$ is adopted without taking mean value, as in (10) and (12), setting $q_i' > 0$ is important to avoid small holes in the results.

ACKNOWLEDGEMENT

This work was supported by the National Natural Science Foundation of China under Grant No. 59937160.

REFERENCES

[1] W. G. Wang, *Ti shi hua ji shu ji qi ying yong*, Publishing house of electronics industry, pp.11, 1998.

[2] S. L. Horowitz, T. Pavlidis, "Picture segmentation by a tree traversal algorithm," *Journal of the Association for Computing Machinery*, vol. 23, pp.368-388, no.2, 1976.

[3] T. Pavlidis, Y. T. Liow, "Integrating region growing and edge detection," *IEEE Trans. Pattern Analysis and Machine Intelligence,* vol. 12, no.3, pp.225-233, 1990.

[4] M. Sonka, S. K. Tadikonda, S. M. Collins, "Knowledge-based interpretation of MR brain images," *IEEE Trans. Medical Imaging*, vol. 15, no.4, pp.443-452, 1996.

[5] I. N. Manousakas, P. E. Undrill, G. G. Cameron, "Split-and-merge segmentation of magnetic resonance medical images: performance evaluation and extension to three dimensions," *Computers and Biomedical Research*, vol.31, pp.393-412, 1998

[6] A. P. Zijdenbos, B. M. Dawant, R. A. Margolin, "Automatic detection of intracranial contours in MR images," *Computerized Medical Imaging and Graphics*, vol. 18, no.1, pp.11-23, 1994

[7] N. Duta, M. Sonka, "Segmentation and interpretation of MR Brain images: an improved active shape model," *IEEE Trans. Medical Imaging*, vol. 17, no. 6, pp.1049-1062, 1998

[8] S. M. Bhandarkat, H. Zhang, "Image segmentation using evolutionary computation," *IEEE Trans. Evolutionary Computation*. Vol 3, no.1, pp.1-21, 1999

[9] Y. A. Tolias, S. M. Panas, "Image segmentation by a fuzzy clustering algorithm using adaptives spatially constrained membership functions," *IEEE Trans. Sys. Man and Cyber. Part A: Sys. And Humans*, vol.28, no.3, pp.359-369

[10] K. S. Cheng, J. S. Lin, C. W. Mao, "The application of competitive Hopfield neural network to medical image segmentation," *IEEE Trans. Med. Imag.*, vol.15, no.4, pp.560-567, 1996

[11] N. Shareef, D. L. Wang, R. Yagel, "Segmentation of medical images using LEGION," *IEEE Trans. Med. Imag.*, vol.18, no.1, pp.74-91, 1999

[12] S. Geman, D. Geman, "Stochastic relaxation, Gibbs distributions, and the Bayesian restoration of images," *IEEE Trans. Pattern Analysis and Machine Intelligence*, vol.PAMI-6, no.6, pp.721-741, 1984

[13] J. Besag, "On the statistical analysis of dirty pictures," J. Roy. Statist. Soc. B, vol.48, no.3, pp.259-302, 1986.

[14] H. Derin, H. Elliott, "Modeling and segmentation of noisy and textured images using Gibbs random fields," *IEEE Trans. Pattern Analysis and Machine Intelligence*, vol. PAMI-9, no.1, pp.39-55, 1987

[15] S. Lakshmanan, H. Derin, "Simultaneous parameter estimation and segmentation of Gibbs random fields using simulated annealing," *IEEE Trans. Pattern Analysis and Machine Intellingence*, vol. 11, no.8, pp.799-813, 1989

[16] Z. Liang, "Tissue classification and segmentation of MR images," *IEEE Engineering in Medicine and Biology*, vol.12, no.1, pp.81-85, 1993

[17] J. C. Rajapakse, J. N. Giedd, J. L. Rapoport, "Statistical approach to segmentation of single-channel cerebral MR images," *IEEE Trans. Med. Imag.*, vol.16, no.2, pp.176-186, 1997

[18] http://www.bic.mni.mcgill.ca/brainweb